Measured propagation characteristics for very-large MIMO at 2.6 GHz

Gao, Xiang; Tufvesson, Fredrik; Edfors, Ove; Rusek, Fredrik

Published in:
[Host publication title missing]

2012

Measured propagation characteristics for very-large MIMO at 2.6 GHz

Xiang Gao, Fredrik Tufvesson, Ove Edfors, Fredrik Rusek
Department of Electrical and Information Technology, Lund University, Lund, Sweden
Email: {xiang.gao, fredrik.tufvesson, ove.edfors, fredrik.rusek}@eit.lth.se

***Abstract*—Very-large multiple-input multiple-output (MIMO), also called massive MIMO, is a new technique that potentially can offer large network capacities in multi-user scenarios, where the base stations are equipped with a large number of antennas simultaneously serving multiple single-antenna users on the same frequency. We investigate channel behavior for a realistic outdoor base station scenario using large arrays. Specifically we compare dirty-paper coding (DPC) capacities and zero-forcing (ZF) sum-rates when using a physically large linear array and a compact cylindrical array, both having 128 antenna elements. As a baseline reference, we use the DPC capacity and ZF sum-rate for the ideal case with independent and identically distributed (i.i.d.) channel coefficients. The investigation shows that the measured channels, for both array types, often allow us to harvest most of the capacities/sum-rates achieved in the i.i.d. case, already at about 10 base station antennas per user.**

I. Introduction

Very-large MIMO systems, also known as massive MIMO or large-scale antenna systems is a new research field in wireless communications. We consider multi-user MIMO (MU-MIMO) where a base station is equipped with a large number (say, tens to hundreds) of antennas as compared to previously considered systems, and is simultaneously serving several single-antenna users on the same frequency. It has been shown in theory that such systems have the potential to remarkably improve performance in terms of link reliability and data rate with simple signal processing schemes [1] [2]. This is due to the important property of very-large MIMO that it has the ability to spatially decorrelate the user channels. The fundamental idea is that as the number of base station antennas grows large, the channel vectors between users and the base station become very long random vectors and under "favorable" propagation conditions, these channel vectors become pairwise orthogonal.

So far the theoretical studies of very-large MIMO rely to a large extent on the "favorable" propagation conditions, and investigations are mostly based on independent and identically distributed (i.i.d.) complex Gaussian (Rayleigh fading) channels. However, when it comes to practice, we need to know whether realistic propagation environments and large antenna array setups can provide enough decorrelation between user channels, and how they will affect the system performance of very-large MIMO. Channel measurements are needed to investigate the performance and behavior in realistic conditions. In [3], we have investigated the properties of measured channels with an indoor base station using a 128-port cylindrical patch array. We showed that the orthogonality of the user channels, in the studied propagation environment, improves with increasing number of antennas at the base station. Already at 20 antennas, the linear precoding schemes can achieve sum-rates very close to the optimal dirty-paper coding (DPC) capacity for two single-antenna users in the measured channels. In [4] and [5], we have studied the channel behavior of very-large MIMO using a 128-element linear array. The most important observation is that the propagation channel can not be seen as wide-sense stationary over this physically large antenna array. Some scatterers are not visible over the whole array, and for scatterers being visible over the whole array, their power contribution may vary considerably. Thus, large-scale fading can be experienced over the array. Another characteristic is that, due to its large aperture, the angular resolution is very high. Recently, another channel measurement campaign with a scalable antenna array consisting of up to 112 elements was reported in [6]. The results showed that despite fundamental differences between the i.i.d. and the measured channels, a large fraction of the theoretical performance gains of large antenna arrays could also be achieved in practice.

Here we study the channel behavior for a realistic outdoor base station scenario using the 128-port cylindrical array as in [3] and the 128-element linear array as in [5]. As mentioned above, the former is a compact array and relatively small in size, while the latter is physically large. From a practical point of view, it is preferable to have a physically compact array with a large number of antennas at the base station. On the other hand, if we make the arrays smaller in size, it brings some drawbacks such as higher antenna correlations. Therefore, we need to compare what performance we can achieve with the different array structures in realistic propagation environments. For a fair comparison, the channel measurements with the two large arrays were performed in the same semi-urban environment. In this study, we use the capacity/sum-rate performance in the downlink as our measure. We calculate the capacity achieved by the optimal but complex DPC technique and also the sum-rate achieved by a more practical linear precoding. Here we focus on linear zero-forcing (ZF) precoding, which shows good performance with limited number of antennas [1]. Specifically, we evaluate the capacity/sum-rate of the two large arrays under different propagation conditions, and compare them with the theoretical performance obtained in the i.i.d. channels. We would like to know, under different propagation conditions, 1) to what extent the performance based on i.i.d. channels can be achieved in the realistic channels, and 2) what

a) Cylindrical array b) Virtual linear array

Fig. 1. Two large antenna arrays at the base station side: a) a cylindrical array with 128 patch antenna elements and b) a virtual linear array with 128 omni-directional antenna positions.

effect the large array structure has on the system performance. To the authors' best knowledge, there has been no published studies so far focusing on the performance comparison of different large array structures in the realistic propagation environments.

The rest of the paper is organized as follows. In Sec. II, we describe the channel measurements using the two large antenna arrays. In Sec. III we continue with a capacity/sum-rate evaluation, where we compare performance of different scenarios, using both i.i.d. and measured channels. Finally we summarize our contributions and draw conclusions in Sec. IV.

II. Channel measurements

In this section, we describe the channel measurements using the two large antenna arrays.

A. Measurement setups

Two channel measurement campaigns were performed with two different large antenna arrays at the base station. Both arrays contain 128 antenna elements and have an adjacent element spacing of half a wavelength at 2.6 GHz. Fig. 1a shows the cylindrical array, having 16 dual-polarized directional patch antennas in each circle and 4 such circles stacked on top of each other, which gives a total of 128 antenna ports. This large antenna array is physically compact with both diameter and height of about 30 cm. Fig. 1b shows the virtual linear array with an omni-directional antenna moving along a rail, in 128 equidistant positions. In comparison, the linear array is physically large and spans 7.3 m in space.

In both measurement campaigns, an omni-directional antenna was used at the user side. Both measurement data were recorded at a center frequency of 2.6 GHz and a signal bandwidth of 50 MHz. With the cylindrical array, measurements were taken with the RUSK LUND channel sounder, while with the linear array, a HP 8720C vector network analyzer was used.

B. Measurement environments

Both channel measurements, using the cylindrical array and the linear array, were carried out outdoors at the E-building of the Faculty of Engineering (LTH), Lund University, Sweden.

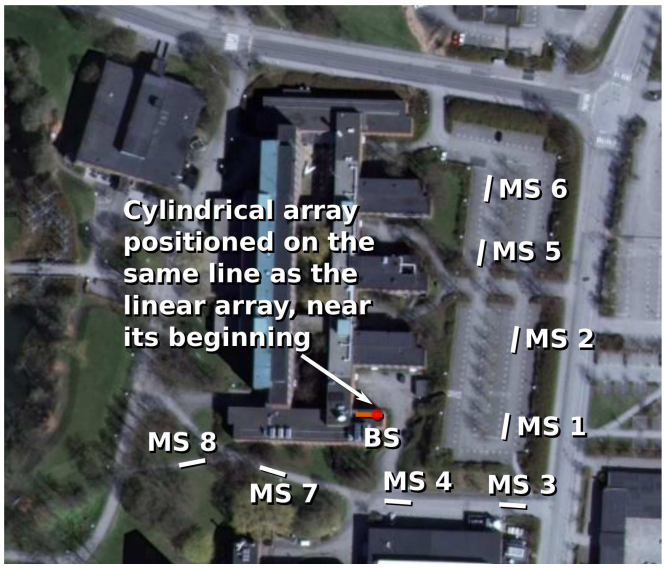

Fig. 2. Overview of the measurement area at the campus of the Faculty of Engineering (LTH), Lund University, Sweden. The two base station antenna arrays were placed on the same roof of the E-building during two measurement campaigns. 8 user sites around the E-building were measured.

Fig. 2 shows an overview of the semi-urban measurement area. The two base station antenna arrays were placed on the roof of the E-building during the two measurement campaigns. More precisely, the cylindrical array was positioned on the same line as the linear array, near its beginning.

At the user side, the omni-directional antenna was moved around at 8 measurement sites (MS) acting as single-antenna users (see Fig. 2). Among these sites, three (MS 1-3) have line-of-sight (LOS) conditions, and four (MS 5-8) have non-line-of-sight (NLOS) conditions, while one (MS 4) has LOS for the cylindrical array, but the LOS component is blocked by the edge of the roof for the linear array. At each site, 5 positions were measured.

To illustrate the propagation characteristics in different scenarios, Fig. 3 shows the angular power spectrum along the linear array for one LOS and one NLOS scenario. The cylindrical array was positioned at the beginning of the linear array, therefore, we can consider that it experiences the directions of arrivals at that part of the linear array. In Fig. 3a, we can see a strong LOS component from 160° and some scatterers at around 20° with varying power contribution. In Fig. 3b, it can be seen that in the NLOS scenario the scatterers are more spread out in space and have significant power variation over the array. As reported in [5], the linear array experiences large-scale fading over the array. Meanwhile the cylindrical array also experiences large power variation over the array, but mainly due to the polarization and directional pattern of its patch antenna elements. This power variation over the antenna arrays can be critical to the performance evaluations of very-large MIMO systems.

Now we consider the differences of two large arrays in terms of angular resolution. The linear array is physically large in

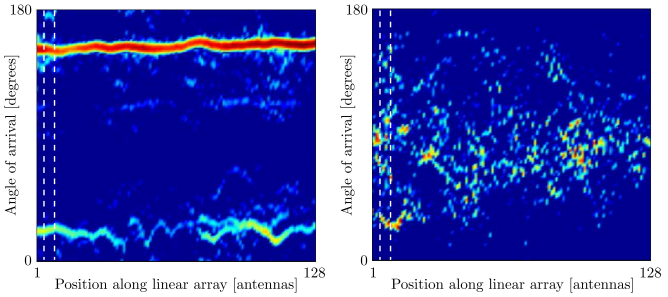

Fig. 3. Angular power spectrum along the 128-element linear array. The dashed lines indicate the position of the cylindrical array. a) A LOS scenario when the user is at MS 2. b) A NLOS scenario when the user is at MS 7.

one dimension, while the cylindrical array is compact but has its antenna elements distributed in two dimensions in space. Therefore, the linear array has superior angular resolution but only in one dimension. The cylindrical array has lower angular resolution, due to its smaller aperture, but it can resolve both azimuth and elevation, which may be an advantage in certain environments.

III. Performance evaluation

In this section, we first describe the calculation of the downlink capacity/sum-rate achieved by dirty-paper coding (DPC) and zero-forcing (ZF) linear precoding. Then we use these to evaluate the performance in the measured channels using the two different large arrays, and compare with the theoretical performance obtained in the i.i.d. channels.

A. DPC capacity and ZF precoding sum-rate

We consider the downlink of a single-cell MU-MIMO system: the base station is equipped with M antennas, and simultaneously serves K single-antenna users. We assume that the base station has perfect channel state information (CSI). The signal model of a narrow-band MIMO channel can be described as

$$\boldsymbol{y} = \sqrt{\frac{\rho K}{M}}\boldsymbol{H}\boldsymbol{z} + \boldsymbol{n}, \tag{1}$$

where $\boldsymbol{H}$ is a normalized $K \times M$ channel matrix, $\boldsymbol{z}$ is the transmit vector across the M antennas, $\boldsymbol{y}$ is the receive vector at the K users, and $\boldsymbol{n}$ is a noise vector with unit variance elements. The variable ρ contains the transmit energy, assuming $\boldsymbol{z}$ satisfies $\mathbb{E}\left\{\|\boldsymbol{z}\|^2\right\} = 1$. The channel matrix is normalized to have unit average energy in its entries over all the frequencies. As can be seen from the term $\rho K/M$, we increase the transmit power with the number of users and reduce it as the number of base station antennas grows. As K increases, we keep the same transmit power per user. With increasing M the array gain increases and we choose to harvest this gain as reduced transmit power instead of increased receive signal-to-noise ratio (SNR) at the users.

The capacity in the MU-MIMO downlink is given as [7],

$$C_{\mathrm{DPC}} = \max_{\boldsymbol{P}} \log_2 \det\left(\boldsymbol{I} + \frac{\rho K}{M}\boldsymbol{H}^H\boldsymbol{P}\boldsymbol{H}\right), \tag{2}$$

which can be achieved by the non-linear dirty-paper coding (DPC) technique. $\boldsymbol{P}$ is a diagonal matrix for power allocation with $P_i, i = 1, 2, ..., K$ on its diagonal. The capacity is found by optimizing over $\boldsymbol{P}$ under the total power constraint $\sum_{i=1}^{K} P_i = 1$. This optimization is done by the sum power iterative waterfilling algorithm in [8].

Less optimal but also less complex strategies are the linear precoding schemes, such as zero-forcing (ZF) and matched filter (MF) precodings. The ZF precoder sets

$$\boldsymbol{z} = \boldsymbol{H}^{+}\sqrt{\boldsymbol{P}}\boldsymbol{x} = \boldsymbol{H}^H\left(\boldsymbol{H}\boldsymbol{H}^H\right)^{-1}\sqrt{\boldsymbol{P}}\boldsymbol{x}, \tag{3}$$

where the superscript "+" denotes the pseudo-inverse of a matrix, and the vector $\boldsymbol{x}$ comprises data symbols for the K users, where each entry has unit average energy. The sum-rate achieved by ZF precoding can be written as [9],

$$C_{\mathrm{ZF}} = \max_{\boldsymbol{P}} \sum_{i=1}^{K} \log_2\left(1 + \frac{\rho K}{M}P_i\right), \tag{4}$$

subject to the total power constraint,

$$\sum_{i=1}^{K} P_i\left[\left(\boldsymbol{H}\boldsymbol{H}^H\right)^{-1}\right]_{i,i} = 1. \tag{5}$$

The optimization of power allocation is solved using the standard waterfilling solution [10].

With the normalizations above and as M goes to infinity, under favorable propagation conditions, the channels to different users become interference free (IF) [1] with per-user SNRs ρ. The limiting capacity we can expect therefore becomes

$$C_{\mathrm{IF}} = K\log_2\left(1 + \rho\right), \tag{6}$$

for equal power distribution among users.

We calculate the capacity/sum-rate for different numbers of base station antennas M in the measured channels and the i.i.d. channels. The global attenuation is removed in the channel matrix, while small-scale and large-scale fading are remaining. This means that we retain the power variations over frequencies and base station antennas. For each M, we randomly select 2000 subsets out of the 128 antennas. For all these subsets, capacities/sum-rates are averaged over the 50 MHz measurement bandwidth. In the i.i.d. channels, there is no difference between the subsets, but in the measured channels with the two different antenna arrays, there is a significant difference between the subsets in terms of power and antenna correlation.

B. Results and discussion

With the available measurements, we can compare many different setups with various numbers of users and combinations on user positions. Of these we have chosen three setups, which we present performance results for and make comparisons between. Each setup has the same number of users, to allow direct comparisons. In two of the setups the users are placed close to each other (1.5-2 m spacing), representing situations where the spatial separation of users is

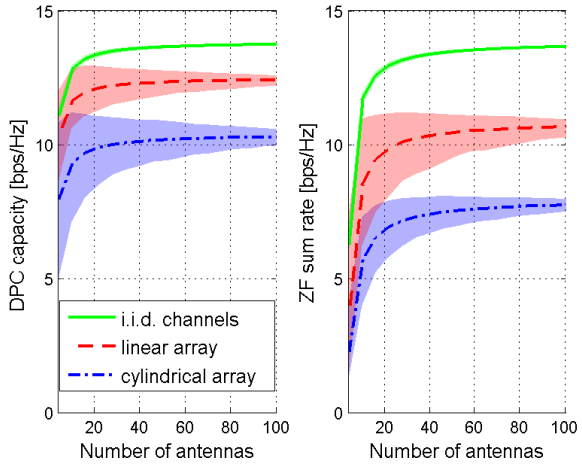

Fig. 4. Four users close to each other at MS 2, with LOS to the base station antenna arrays.

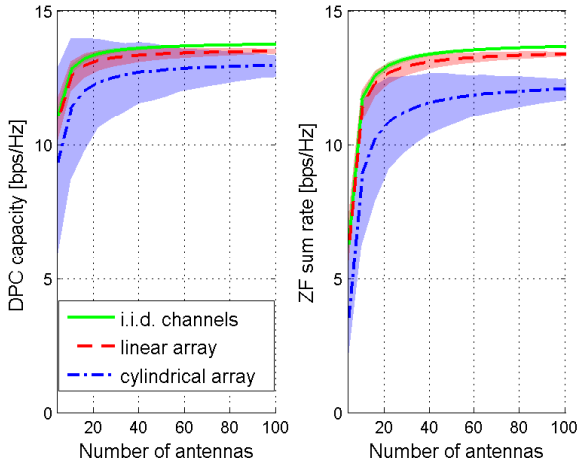

Fig. 5. Four users close to each other at MS 7, without LOS to the base station antenna arrays.

particularly difficult. In the first of these setups the users have LOS to the base station, while for the other they do not. In the third setup, the users are well separated from each other (>10 m spacing), but all have channels with LOS characteristics. In all three setups, we have selected the interference-free SNR to $\rho = 10$ dB. We show both average DPC capacities and ZF sum-rates, as well as the 5%-95% regions, for 2000 random antenna selections, when using between 4 and 100 base station antennas.

The DPC capacity and the ZF sum-rate for a particularly difficult setup is shown in Fig. 4, where the users are closely spaced and have LOS to the base station. We observe that for the i.i.d. channels both the DPC capacity and the ZF sum-rate converge to that of the interference free case in (6), $K \log_2(1+\rho) = 4 \log_2(1+10) = 13.8$ bps/Hz. The variation for the i.i.d channels is very low across the entire range of base station antennas. At low numbers of antennas this is mostly due to the average over a 50 MHz bandwidth. For higher numbers of base station antennas it is also influenced by the fact that when selecting 100 of 128 antennas, at least 72 antennas are in common between any pair of selections. For the linear and cylindrical arrays, however, the averages are significantly lower and the variations are larger. The performance of the cylindrical array is significantly lower than that of the linear array and, when going from DPC (left plot) to linear ZF precoding (right plot), there is a significant additional drop in the performance. Despite all this, even the worst combination of cylindrical array and ZF precoding performs at about 55% of the ideal i.i.d. DPC capacity, when the number of antennas is above 40.

In Fig. 5 we have a setup where the users are still closely spaced, like above, but now without LOS to the base station antenna arrays. The NLOS condition with rich scattering as shown in Fig. 3b should improve the situation, by providing more "favorable" propagation and thus allowing better spatial separation of the users. The effect of this is clearly seen in the plots in Fig. 5, especially when comparing with those in Fig. 4. Despite the closely spaced users, the linear array here provides close to optimal performance both for DPC and ZF precoding, while the cylindrical array reach more than 90% and 80% with DPC and ZF precoding, respectively.

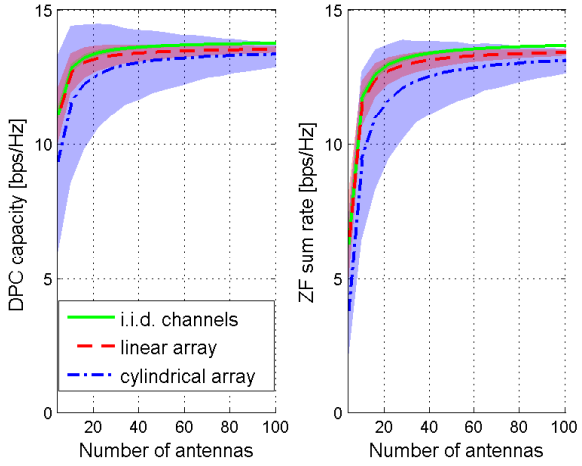

Fig. 6. Four users well separated at MS 1-4, each has LOS condition except the one at MS 4 for the linear array.

In the last setup, the four users all have LOS characteristics in their channels, but are well separated. The increased separation should help to improve the performance. The results are shown in Fig. 6. We now observe that both linear and cylindrical arrays perform close to that of the ideal i.i.d. DPC capacity, except for very low numbers of antennas in combination with ZF precoding. Using the linear array, as few as 20 antennas gives very competitive performance, while slightly higher numbers are required for the cylindrical array.

Throughout the three setups discussed above and whose performances are shown in Fig. 4 - Fig. 6, we observe that the variations in capacity/sum-rate are larger for the cylindrical

array than for the linear array. The small physical size of the cylindrical array should make the large-scale fading it experiences, caused by the environment, smaller than that experienced by the physically much larger linear array. A remaining explanation of the variations is the difference in directivity and polarization of the antenna elements in the two arrays. The linear array has omni-directional antenna elements, with the same (vertical) polarization as the user antenna, while the cylindrical array has directional patch antenna elements with both horizontal and vertical polarization. The variations introduced by the antenna element characteristics seem to have a larger impact on the performance variations than large-scale fading caused by the environment where the measurements were performed.

IV. Summary and conclusions

The presented investigation shows that in a realistic propagation environment we have characteristics that allow for efficient use of very-large MIMO technology. We have shown and compared capacity/sum-rate results for different precoders, using both ideal i.i.d. channels and measured real channels, for the case of four users.

In the most difficult situation studied, closely spaced users with LOS to the base station, even the worst combination of cylindrical array and linear ZF precoding reach about 55% of the ideal i.i.d. channel DPC capacity. In the other cases, both the linear and cylindrical arrays can reach above 80-90% of the ideal performance, even with simple linear ZF precoding. The limit for "large" MIMO, in terms of number of base station antennas, seems to be in a reasonable range of about 10 times the number of users. Beyond that point very little extra performance is observed in our measured channels.

The presented capacity/sum-rate results show that most of the predicted capacity gains of very-large MIMO are possible to harvest already at reasonable number of antennas, using simple linear precoding, for measured channels in a realistic scenario.

Acknowledgement

The authors would like to acknowledge the support from ELLIIT – an Excellence Center at Linköping-Lund in Information Technology.

References

[1] F. Rusek, D. Persson, B. K. Lau, E. G. Larsson, T. L. Marzetta, O. Edfors, and F. Tufvesson, "Scaling up MIMO: Opportunities and challenges with very large arrays," *IEEE Signal Processing Magazine*, Jan. 2013.

[2] T. L. Marzetta, "Noncooperative cellular wireless with unlimited numbers of base station antennas," *IEEE Transactions on Wireless Communications*, vol. 9, no. 11, pp. 3590–3600, Nov. 2010.

[3] X. Gao, O. Edfors, F. Rusek, and F. Tufvesson, "Linear pre-coding performance in measured very-large MIMO channels," in *2011 IEEE Vehicular Technology Conference (VTC Fall)*, Sep. 2011, pp. 1–5.

[4] S. Payami and F. Tufvesson, "Channel measurements and analysis for very large array systems at 2.6 GHz," in *2012 6th European Conference on Antennas and Propagation (EUCAP)*, Mar. 2012, pp. 433–437.

[5] X. Gao, F. Tufvesson, O. Edfors, and F. Rusek, "Channel behavior for very-large MIMO systems - initial characterization," in *COST IC1004, Bristol, UK*, Sep. 2012.

[6] J. Hoydis, C. Hoek, T. Wild, and S. ten Brink, "Channel measurements for large antenna arrays," in *2012 International Symposium on Wireless Communication Systems (ISWCS)*, Aug. 2012, pp. 811–815.

[7] S. Vishwanath, N. Jindal, and A. Goldsmith, "Duality, achievable rates, and sum-rate capacity of Gaussian MIMO broadcast channels," *IEEE Transactions on Information Theory*, vol. 49, no. 10, pp. 2658–2668, Oct. 2003.

[8] N. Jindal, W. Rhee, S. Vishwanath, S. Jafar, and A. Goldsmith, "Sum power iterative water-filling for multi-antenna Gaussian broadcast channels," *IEEE Transactions on Information Theory*, vol. 51, no. 4, pp. 1570–1580, Apr. 2005.

[9] A. Wiesel, Y. Eldar, and S. Shamai, "Zero-forcing precoding and generalized inverses," *IEEE Transactions on Signal Processing*, vol. 56, no. 9, pp. 4409–4418, Sep. 2008.

[10] T. Cover and J. Thomas, *Elements of Information Theory*. Wiley, New York, 1991.